

# A DUAL LEAST-SQUARES FINITE ELEMENT METHOD FOR LINEAR HYPERBOLIC PDES: A NUMERICAL STUDY

LUKE OLSON<sup>†‡§</sup>

**Abstract.** In this paper, we develop a least-squares finite element method for linear Partial Differential Equations (PDEs) of hyperbolic type. This formulation allows for discontinuities in the numerical approximation and yields a linear system which can be handled efficiently by Algebraic Multigrid solvers.

We pose the classical advection equation as a “dual”-type problem and relate the formulation to previous attempts. Convergence properties and solution quality for discontinuous solutions are investigated for standard, conforming finite element spaces on quasi-uniform tessellations of the domain and for the general case when the flow field is not aligned with the computational mesh. Algebraic Multigrid results are presented for the linear system arising from the discretization and we study the success of this solver.

**Key words.** least-squares variational formulation, finite element discretization, hyperbolic problems, multigrid

**AMS subject classifications.** 65N15, 65N30, 65N55

**1. Introduction.** We consider linear Partial Differential Equations (PDEs) of hyperbolic type that are of the form

$$\nabla \cdot (\mathbf{b}u) = f \quad \text{in } \Omega, \quad (1.1)$$

$$u = g \quad \text{on } \Gamma_I, \quad (1.2)$$

with  $\mathbf{b}(\mathbf{x})$  a flow field on  $\Omega \subset \mathbb{R}^2$ , and

$$\Gamma_I := \{\mathbf{x} \in \partial\Omega : \mathbf{n}(\mathbf{x}) \cdot \mathbf{b}(\mathbf{x}) < 0\}, \quad (1.3)$$

the inflow part of the boundary of domain  $\Omega$ . Here,  $\mathbf{n}(\mathbf{x})$  is the outward unit normal of  $\partial\Omega$ . For this paper we assume that (1.1) represents a conservation law and consider  $f = 0$ . For a large class of forcing terms,  $f$ , we can use a modified lifting argument that results in solving an auxiliary problem. However, we leave this discussion to another paper.

Given  $\Omega$  in (1.1-1.2)  $\subset \mathbb{R}^2$ ,  $\mathbf{b}(\mathbf{x}) = (b_1(\mathbf{x}), b_2(\mathbf{x}))$  describes a vector field on  $\Omega$ . We make the following assumptions on  $\mathbf{b}$ : for any  $\mathbf{x}_i \in \Gamma_I$ , let  $\mathbf{x}(r) = (x(r), y(r))$  be a streamline of  $\mathbf{b}$ , that is, the solution of

$$\frac{dx(r)}{dr} = b_1(\mathbf{x}(r)), \quad \frac{dy(r)}{dr} = b_2(\mathbf{x}(r)), \quad (1.4)$$

with initial condition  $\mathbf{x}(r_0) = \mathbf{x}_i$ . Let  $\beta = |\mathbf{b}|$  and assume there exists constants  $\beta_0$  and  $\beta_1$  such that  $0 < \beta_0 \leq \beta \leq \beta_1 < \infty$  on  $\Omega$ . We assume that there is a transformation to a coordinate system  $(r, s)$  such that the streamlines are lined up with the  $r$  coordinate direction and the Jacobian,  $J$ , of the transformation is bounded. This implies that no two streamlines intersect and that  $\Omega$  is the collection of all such streamlines. Further, we assume that every streamline connects  $\Gamma_I$  and  $\Gamma_O$  with a finite length  $\ell(\mathbf{x}_i)$ , where  $\mathbf{x}_i \in \Gamma_I$ . We consider piecewise continuous boundary data,  $g$  in (1.2). Generally, we then assume  $g \in H^{\frac{1}{2}-\varepsilon}(\Gamma_I)$ .

We require partition  $\mathcal{T}^h$  of  $\Omega$  to be an admissible, quasi-uniform tessellation (see [4, 6]). We assume the same for  $\hat{\mathcal{T}}^h$  of  $\hat{\Omega}$ , the image of  $\mathcal{T}^h$  under the transformation described above. For our numerical tests, we use a uniform partition of quadrilaterals.

Equations of the type (1.1-1.2), are considered a prototype equation for more general equations of hyperbolic type. The equations are found in a wide variety of applications including systems of conservation laws [9, 16, ?, ?], which we briefly consider in this paper. Nonlinear conservation laws, which represent a large class of applications based on our model equations, fit well into our proposed framework, but we limit the discussion in this paper to the linear case.

Numerical methods for solving PDEs of hyperbolic type have, until recently, been dominated by finite volume methods. Finite element methods have been gaining popularity for this class of problems and we

<sup>†</sup>Department of Applied Mathematics, Campus Box 526, University of Colorado at Boulder, Boulder, CO 80302

<sup>‡</sup>luke.olson@colorado.edu <http://amath.colorado.edu/student/olsonln/>

<sup>§</sup>Research in collaboration with Hans De Sterck, Tom Manteuffel and Steve McCormick.

propose a discretization in this setting. Continuous and discontinuous Galerkin and Streamline-Upwind Petrov-Galerkin (SUPG) based methodologies have been previously considered (see [8, 12, 19, 13, 15, 14]). A common theme in these frameworks has been the addition of least-squares terms for stabilization. Solution quality is degraded in the form of spurious oscillations and widespread smearing without least-squares stabilization terms. A comparison of Galerkin, SUPG and LSFEM for convection problems can be found in [3].

In [10], we studied Least-Squares Finite Element Methods (LSFEM) for (1.1-1.2). In particular, we considered problems with discontinuous solutions and investigated the finite-element convergence extensively for several finite element spaces and least-squares formulations. The main results in [10] include a formal characterization of a conforming and nonconforming finite element methods based on a least-squares minimization principle. Moreover, we found encouraging Algebraic Multigrid results using this approach. This is the emphasis of our current research: to appropriately discretize PDEs of hyperbolic type and efficiently solve the resulting system in a multilevel setting.

As we described in [10], least-squares methods are naturally attractive variational formulations. If the formulation can be shown to be well posed, then well-posedness of the discrete problem follows immediately. The least-squares setting leads to symmetric, positive-definite linear systems. Further, least-squares methods provide a sharp, straightforward *a posteriori* error estimator [1] for use in adaptive algorithms. In this paper, we adhere to the least-squares methodology in order to maintain these general, advantageous properties.

We consider discontinuous solutions to (1.1-1.2) in this paper. Discontinuities in the prescribed boundary data,  $g$  on  $\Gamma_I$ , will be propagated along the characteristics across the domain. We seek to resolve these discontinuities in our numerical approximation and we pose the PDE as a “dual”-type problem. In a least-squares setting, we use a conforming finite element space of continuous bilinear elements to approximate the “dual” variable. We will see that this formulation allows for discontinuities in the discrete approximation to  $u$ , the “primal” variable. Furthermore, we find efficient Algebraic Multigrid performance for linear systems that arise from this formulation.

The paper is organized as follows. In this section, we describe the standard notation used throughout the paper. In Section 2.1, we propose a new “dual”-type formulation of (1.1-1.2) and discuss the implications of such a setting. In Sections 3 and 4, we present numerical evidence. We study the convergence of the finite element discretization and Algebraic Multigrid performance, respectively. We leave concluding remarks and extensions of this framework to Section 5.

*Remark.* Although we use the term “dual” frequently throughout the paper, this should not be confused with the idea of using a dual space as is used in the so-called FOSLL method.

**1.1. Nomenclature.** First, we establish the notation we will use throughout the paper. We use the standard definition and notation for a Sobolev space  $H^k(\Omega)^d$  for  $k \geq 0$  and its associated inner product and norm,  $\langle \cdot, \cdot \rangle_k$  and  $\| \cdot \|_k$ , respectively. In the case of  $k = 0$ , we will use  $L^2(\Omega)^d$  to denote the space and  $(\cdot, \cdot)$  and  $\| \cdot \|$  for the  $L^2$  inner product and norm respectively.  $H_0^k(\Omega)$  will denote the closure for the  $\| \cdot \|_k$ -norm of the linear space of infinitely differentiable function with compact support on  $\Omega$ .

We define the curl operator and its formal adjoint in 2-D by considering the **curl** in 3-D,

$$\mathbf{curl} = \nabla \times = \begin{bmatrix} 0 & -\partial_z & \partial_y \\ \partial_z & 0 & -\partial_x \\ -\partial_y & \partial_x & 0 \end{bmatrix}. \quad (1.5)$$

From the dotted lines in (1.5), we define for distribution  $p$  and vector distribution  $\mathbf{w}$ ,

$$\mathbf{curl} p = \nabla^\perp p = \begin{pmatrix} \partial_y p \\ -\partial_x p \end{pmatrix}, \quad (1.6)$$

$$\mathbf{curl} \mathbf{w} = \nabla \times \mathbf{w} = \partial_x w_2 - \partial_y w_1. \quad (1.7)$$

Finally, we define  $\text{div} \equiv \nabla \cdot$  in the standard way and let

$$H(\Omega, \mathbf{grad}) = \{p \in L(\Omega) : \nabla p \in L^2(\Omega)^2\}, \quad (1.8)$$

$$H(\Omega, \mathbf{curl}) = \{p \in L(\Omega) : \nabla^\perp p \in L^2(\Omega)^2\}, \quad (1.9)$$

$$H(\Omega, \text{div}) = \{\mathbf{w} \in L(\Omega)^d : \nabla \cdot \mathbf{w} \in L^2(\Omega)\} \quad (1.10)$$

be a Hilbert spaces with the respective norms

$$\|p\|_{H(\Omega, \mathbf{grad})} := (\|p\|^2 + \|\nabla p\|^2)^{\frac{1}{2}}, \quad (1.11)$$

$$\|p\|_{H(\Omega, \mathbf{curl})} := (\|p\|^2 + \|\nabla^\perp p\|^2)^{\frac{1}{2}}, \quad (1.12)$$

$$\|\mathbf{w}\|_{H(\Omega, \mathbf{div})} := (\|\mathbf{w}\|^2 + \|\nabla \cdot \mathbf{w}\|^2)^{\frac{1}{2}}. \quad (1.13)$$

**1.2. Least-Squares Functional.** In [10], we pose (1.1-1.2) as a least-squares minimization principle for divergence-free flow fields  $\mathbf{b}(\mathbf{x})$ . For the PDE,

$$\mathbf{b} \cdot \nabla u = f \quad \text{in } \Omega, \quad (1.14)$$

$$u = g \quad \text{on } \Gamma_I, \quad (1.15)$$

we posed the problem as the minimization of the least-squares functional

$$\mathcal{F}(u; f, g) := \|\mathbf{b} \cdot \nabla u - f\|_0^2 + \|u - g\|_B^2, \quad (1.16)$$

where

$$\|g\|_B^2 := \int_{\Gamma_I} |\mathbf{n}_\mathbf{b} \cdot \mathbf{n}_{\Gamma_I}| g^2 ds. \quad (1.17)$$

Here,  $\mathbf{n}_\mathbf{b}$  is the unit normal in the direction of  $\mathbf{b}$  and  $\mathbf{n}_{\Gamma_I}$  is the outward unit normal on the boundary  $\Gamma_I$ .

The finite elements used in [10] were both continuous and discontinuous piecewise polynomials. We found the numerical approximation to adequately resolve the discontinuity in the solution. Furthermore, using an Algebraic Multigrid method to solve the resulting linear system, the complexity grew slowly relative to the number of unknowns. In this paper, we formulate a “dual” problem to allow discontinuities in the approximate solution and we focus on improving the multigrid performance.

**2. “Dual” least-squares formulation.** In this section we pose (1.1-1.2) as a least-squares minimization principle. We will see in the following discussion that the least-squares formulation in this “dual” approach allows for solutions of low regularity. This is particularly useful for (1.1-1.2), where boundary data  $g(\mathbf{x}) \in H^{\frac{1}{2}-\varepsilon}(\Omega)$  results in possible discontinuities in the solution throughout the domain. We refer to [10, 9] for a more complete characterization of the hyperbolic problem in this respect.

**2.1. Setup.** We begin by writing (1.1-1.2) as

$$\nabla \cdot (\mathbf{w}) = 0 \quad \text{in } \Omega, \quad (2.1)$$

$$\mathbf{w} = \mathbf{b}u \quad \text{in } \Omega, \quad (2.2)$$

$$\mathbf{w} = \mathbf{b}g \quad \text{on } \Gamma_I. \quad (2.3)$$

From this viewpoint, a natural finite element choice for  $\mathbf{w} \in H(\Omega, \mathbf{div})$  are the so-called Raviart-Thomas finite elements [4]. Consider the 2-D exactness sequence discussed in detail in [2]. Let

$$\mathcal{W}^{\mathbf{grad}} = \text{finite element subspace of } H_0(\Omega, \mathbf{grad}), \quad (2.4)$$

$$\mathcal{W}^{\mathbf{curl}} = \text{finite element subspace of } H_0(\Omega, \mathbf{curl}), \quad (2.5)$$

$$\mathcal{W}^{\mathbf{div}} = \text{finite element subspace of } H_0(\Omega, \mathbf{div}), \quad (2.6)$$

$$\mathcal{W}^{L^2} = \text{finite element subspace of } L^2(\Omega). \quad (2.7)$$

For these subspaces we have the sequences

$$\mathcal{W}^{\mathbf{grad}} \xrightarrow{\nabla^\perp} \mathcal{W}^{\mathbf{div}} \xrightarrow{\nabla \cdot} \mathcal{W}^{L^2}, \quad (2.8)$$

$$\mathcal{W}^{\mathbf{grad}} \xrightarrow{\nabla} \mathcal{W}^{\mathbf{curl}} \xrightarrow{\nabla^\perp} \mathcal{W}^{L^2}. \quad (2.9)$$

Denote the space  $\mathcal{W}^{\text{div}}$  as the space of Raviart-Thomas finite elements or  $RT^h$ . A divergence-free subspace  $C^h \subset RT^h$  can be constructed from  $\phi \in \mathcal{W}^{\text{grad}}$  by  $\nabla^\perp \phi$  [11]. Thus, if we choose Raviart-Thomas elements of the form  $\mathbf{w}^h = \nabla^\perp \phi = \begin{pmatrix} -\phi_y \\ \phi_x \end{pmatrix}$ , then  $\nabla \cdot \mathbf{w}^h = 0$  and (2.1) is immediately satisfied.

Notice that  $\mathbf{b}^\perp \cdot \mathbf{w} = \mathbf{b}^\perp \mathbf{b}u = 0$  from (2.2). Then (2.1-2.3) becomes

$$\nabla \cdot \mathbf{w} = 0 \quad \text{in } \Omega, \quad (2.10)$$

$$\mathbf{b}^\perp \cdot \mathbf{w} = 0 \quad \text{in } \Omega, \quad (2.11)$$

$$\mathbf{w} = \mathbf{b}g \quad \text{on } \Gamma_I. \quad (2.12)$$

We pose (2.10-2.12) as the minimization of the least-square functional

$$\tilde{\mathcal{G}}(\mathbf{w}; g) := \|\nabla \cdot \mathbf{w}\|_{0,\Omega}^2 + \|\mathbf{b}^\perp \cdot \mathbf{w}\|_{0,\Omega}^2 + \|\mathbf{w} - \mathbf{b}g\|_{0,\Gamma_I}^2. \quad (2.13)$$

If we use face elements for  $\mathbf{w}$  in the associated weak problem, then we could equally consider the functional

$$\hat{\mathcal{G}}(\mathbf{w}; g) := \|\mathbf{b}^\perp \cdot \mathbf{w}\|_{0,\Omega}^2 + \|\mathbf{w} - \mathbf{b}g\|_{0,\Gamma_I}^2, \quad (2.14)$$

since  $\nabla \cdot \mathbf{w} = 0$ . From the exact sequence (2.8), we know that if  $\nabla \cdot \mathbf{w} = 0$ , then  $\mathbf{w} = \nabla^\perp p$  for some  $p \in \mathcal{W}^{\text{grad}}$ . The problem then becomes

$$q = \underset{p \in \mathcal{W}^{\text{grad}}}{\text{argmin}} \mathcal{G}(p; g), \quad (2.15)$$

where

$$\mathcal{G}(p; g) := \|\mathbf{b}^\perp \cdot \nabla^\perp p\|_{0,\Omega}^2 + \|\mathbf{w} - \mathbf{b}g\|_{0,\Gamma_I}^2, \quad (2.16)$$

$$= \|\mathbf{b} \cdot \nabla p\|_{0,\Omega}^2 + \|\mathbf{w} - \mathbf{b}g\|_{0,\Gamma_I}^2. \quad (2.17)$$

$$(2.18)$$

We will use the space of continuous piecewise bilinears for the finite element subspace  $\mathcal{W}^{\text{grad}}$  in our numerical computation presented in Section 3.

For  $u$ , we have

$$\mathbf{b}u = \mathbf{w} = \nabla^\perp p. \quad (2.19)$$

In Section 3, we choose to obtain  $u$  directly by

$$u = \frac{1}{|\mathbf{b}|^2} \mathbf{b} \cdot \nabla^\perp p = \frac{1}{|\mathbf{b}|^2} \mathbf{b}^\perp \cdot \nabla p \quad (2.20)$$

This approach clearly allows discontinuities in  $u$ . From (2.20), since  $p$  is piecewise bilinear and continuous across elements,  $u$  may have discontinuities perpendicular to the flow. We can also pose  $\mathbf{b}u = \nabla^\perp p$  as a minimization principle over the space of piecewise constants coupled with the functional defined in (2.16), but we leave this formulation for future analysis.

Finally, define the functional norm as

$$\|p^h\|_{\mathcal{G}} := \sqrt{\mathcal{G}(p^h; 0)}. \quad (2.21)$$

**2.2. Systems.** We can further extend the motivation in Section 2.1 to systems of conservation laws. Let

$$\mathbf{U} = \begin{pmatrix} u_1 \\ u_2 \\ \vdots \\ u_m \end{pmatrix}, \quad (2.22)$$

and  $\nabla \cdot$  be the component-wise version of the div operator discussed in the previous sections. That is, for  $\mathbf{U}, \mathbf{V} \in (H_0^1(\Omega))^m$  and defined by (2.22), let

$$\nabla \cdot \begin{pmatrix} \mathbf{U} \\ \mathbf{V} \end{pmatrix} = \begin{pmatrix} \partial_x u_1 + \partial_y v_1 \\ \partial_x u_2 + \partial_y v_2 \\ \vdots \\ \partial_x u_m + \partial_y v_m \end{pmatrix}. \quad (2.23)$$

We can similarly write a system of hyperbolic PDEs as

$$\nabla \cdot \begin{pmatrix} \mathbf{U} \\ \mathbb{A}\mathbf{U} \end{pmatrix} = \mathbf{0} \quad (2.24)$$

$$u_j = g_j \quad \text{on } \Gamma_{I,j} \text{ for } j = 1, \dots, m. \quad (2.25)$$

In this paper, we consider diagonalizable matrices  $\mathbb{A}$ . Although this simplifies our model, conservation laws of type (2.24) with diagonalizable  $\mathbb{A}$  still constitute a large class of problems. Again, write

$$\begin{pmatrix} \mathbf{U} \\ \mathbb{A}\mathbf{U} \end{pmatrix} = \nabla^\perp \mathbf{P} := \begin{pmatrix} \partial_y \mathbf{P} \\ -\partial_x \mathbf{P} \end{pmatrix} \quad (2.26)$$

The least-squares formulation follows closely to the discussion in Section 2.1. We find numerical results for diagonalizable systems similar to the results presented for the scalar case in Sections 3 and 4.

**3. Numerical Results: Finite Elements.** In this section we numerically study the convergence of the finite element discretization. We discuss the effectiveness of the “dual” least-squares formulation by demonstrating properties of the numerical approximation including contained oscillations and limited smearing. We avoid using a flow aligned mesh and consider an admissible, quasi-uniform tessellation  $\mathcal{T}^h$  of  $\Omega$  (c.f. [4]).

Consider (2.10-2.12) and let  $\Omega = [0, 1] \times [0, 1]$ . Since our goal is a method where the computational grid is independent of the flow, and thus the discontinuity, we investigate a variety of flow fields. Our model example will be the scalar advection problem with

$$\mathbf{b}(\mathbf{x}) = (\cos \theta, \sin \theta), \quad (3.1)$$

where  $\theta$  is the angle the flow makes with the first coordinate axis (for N=2-D). The inflow boundary defined by (1.3) is  $\Gamma_I = (\{0\} \times [0, 1]) \cup ([0, 1] \times \{0\})$ —i.e. the west and south boundaries of the unit square. The prescribed discontinuous boundary data will be

$$g(0, y) = 1.0 \quad \text{for } y \in [0, 1], \quad (3.2)$$

$$g(x, 0) = 0.0 \quad \text{for } x \in [0, 1]. \quad (3.3)$$

With this boundary data, the exact solution is discontinuous with 1.0 above the characteristic emanating from the origin and 0.0 below the characteristic. For the tessellation  $\mathcal{T}^h$  of  $\Omega$  we choose a uniform partition of quadrilaterals. The weak problem associated with the minimization of the least-square functional (2.16) is

Find  $p \in \mathcal{W}^{\text{grad}}$  such that

$$\langle \mathbf{b} \cdot \nabla p, \mathbf{b} \cdot \nabla q \rangle_{0,\Omega} + \langle \nabla^\perp p, \nabla^\perp q \rangle_{0,\Gamma_I} = F(q) \quad \forall q \in \mathcal{W}^{\text{grad}}, \quad (3.4)$$

where

$$F(q) = \langle f, \mathbf{b} \cdot \nabla q \rangle_{0,\Omega} + \langle \mathbf{b}g, \nabla^\perp q \rangle_{0,\Gamma_I}. \quad (3.5)$$

As discussed in Section 2.1, we use continuous bilinear finite elements for  $\mathcal{W}^{\text{grad}}$  resulting in face elements for the variable  $\mathbf{w} = \mathbf{b}u$ .

Table 3 shows the convergences rates of the  $\mathcal{G}$ -norm defined by (2.21) for the error in  $p$  and the convergence rate of the  $L^2$ -norm of the error in  $u$ . Let  $e_p = p - p^h$  and  $e_u = u - u^h$  define the errors. Numerically

$\theta$	$\ e_p\ _{\mathcal{F}}$			$\ e_u\ _0$
	Interior	Boundary	Total	Total
$\frac{\pi}{4}$	0.81	0.50	> 0.50	0.24
$\frac{\pi}{6}$	0.82	0.50	> 0.50	0.26
$\frac{\pi}{8}$	0.83	0.50	> 0.50	0.28
$\frac{\pi}{12}$	0.85	0.50	> 0.50	0.32

TABLE 3.1

Convergence rates,  $\alpha$ , for the functional norm of  $e_p = p - p^h$  and  $L^2$ -norm of  $e_u = u - u^h$ .

we observe the convergence rate of  $\|e_u\|_0$  to be close to the discretization results for the functional defined in (1.16), c.f. [10]. Furthermore, due to the increased regularity in  $p$ , we find attractive convergence results in the functional norm for the “dual” variable  $p$ . The convergence is dominated by the rate of convergence on the boundary, as expected. Nevertheless, the order clearly remains above  $\frac{1}{2}$  for these test problems.

Solution quality is also high. Figure 3.1 shows contour plots for various angles  $\theta$ . The smearing around the discontinuity in the approximate solution is well contained and comparable to the results reported in [3]. Moreover, the second plot of Figure 3.2 shows the overshoot and undershoot for the solution. For brevity, we only present the case of  $N = 32$  and  $\theta = \frac{\pi}{8}$  since this profile is representative of other test angles and mesh sizes. Finally, the first plot of Figure 3.2 reveals what we expected from this formulation. The numerical approximation to  $u$  contains discontinuities and we visually confirm that this approximation is an adequate representation of the solution.

**4. Numerical Results: AMG.** In this section we discuss solution of the linear system arising from the finite element discretization developed above. Although the minimization problem is not  $H^1$  equivalent, an advantageous property found in many formulations of elliptic PDEs, we will focus on multigrid iterative solvers. In particular, we consider the Brandt-McCormick-Ruge Algebraic Multigrid method [5] with a variety of interpolation techniques. We test the convergence of AMG using the example flow described in Section 3. All calculations are done using John Ruge’s FOSPACK (First-Order Systems Least-Squares Finite Element Software Package) [17]. For an overview of multigrid methods see [20, 7].

A point-wise Gauss-Seidel sweep is used for relaxation on each level. First, the fine grid points and then the coarse grid points are relaxed on the down sweep of a cycle, while coarse grid points are relaxed before fine grid points using reverse ordering on the up sweep of a cycle. This ensures a symmetric process.

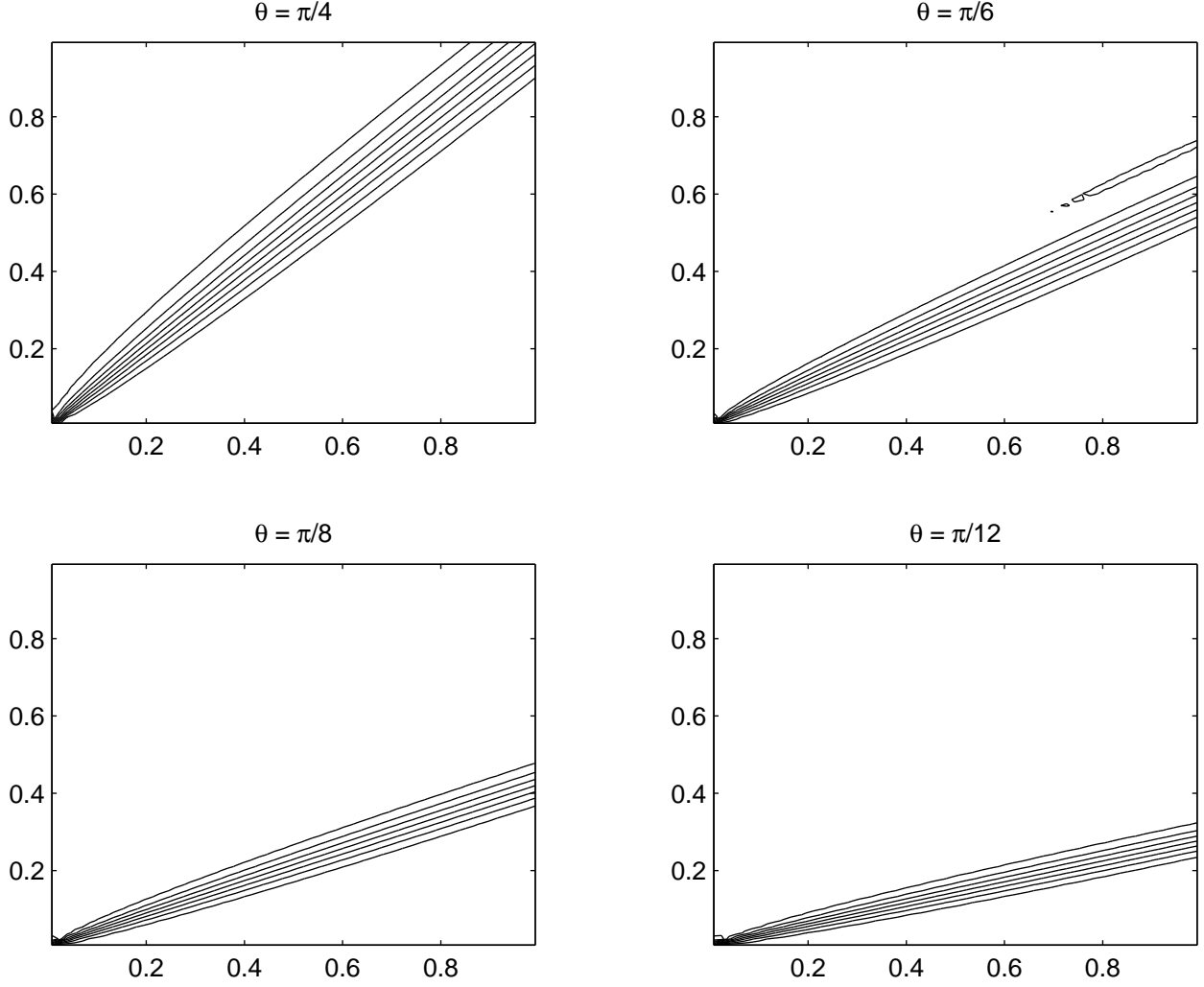
Table 4.1 shows a summary of the AMG performance. Column 1 is the angle  $\theta$  described in (3.1) and Column 2 lists the problem size—i.e. the number of elements—in each coordinate direction. Column 3 displays the number of W(1,1)-cycles needed to obtain a relative residual less than a tolerance of  $1.0e - 10$  and we confirm our results using a zero right-hand-side. As a measure of complexity, we compute the work per cycle in terms of fine-grid relaxation sweeps. The cycle complexity,  $W_c$ , is defined to be the total number of nonzero matrix entries on each level times the number of relaxation sweeps performed on that level divided by the number of nonzero entries in the fine grid matrix. This represents the work per cycle relative to the work on the fine grid. Table 4.1 shows these values to remain fairly constant, particularly for finer mesh sizes. We also present the convergence factor,  $\rho$ , in the table as it will be needed to compute the work units per digit of accuracy in the final column. The convergence factors for this problem are impressive, but do not completely determine the performance of the algorithm as a whole, especially when using W-cycles. To obtain an accumulative view of the AMG performance we investigate the work units per digit accuracy. The work units required to reduce the error by a factor of 10 is computed as

$$W_d = -\frac{W_c}{\log \rho}. \quad (4.1)$$

Notice in Column 6 of Table 4.1 that the work units per digit accuracy appear to remain constant even for larger problem. This suggests that the AMG algorithm is indeed performing independent of the grid size.

Recall the weak form of minimization of

$$\mathcal{G}(p; g) := \|\mathbf{b}^\perp \cdot \nabla^\perp p\|_{0,\Omega}^2 + \|\nabla^\perp p - \mathbf{b}g\|_{0,\Gamma_I}^2, \quad (4.2)$$

FIG. 3.1. Contour plots for different test angles,  $\theta$ .

find  $p \in \mathcal{W}^{\text{grad}}$  such that

$$\langle \mathbf{b} \cdot \nabla p, \mathbf{b} \cdot \nabla q \rangle_{0,\Omega} + \langle \nabla^\perp p, \nabla^\perp q \rangle_{0,\Gamma_I} = F(q) \quad \forall q \in \mathcal{W}^{\text{grad}}, \quad (4.3)$$

where  $F(q) = \langle f, \mathbf{b} \cdot \nabla q \rangle_{0,\Omega} + \langle \mathbf{b}g, \nabla^\perp q \rangle_{0,\Gamma_I}$ .

The discrete form of (4.3) is similar to the discrete Galerkin approximation of highly anisotropic diffusion. To see this, write  $M = I = \mathbf{s}\mathbf{s}^T + \mathbf{t}\mathbf{t}^T$  where  $\mathbf{s} \cdot \mathbf{s} = 1$ ,  $\mathbf{t} \cdot \mathbf{t} = 1$  and  $\mathbf{s} \cdot \mathbf{t} = 0$ . When  $A = \mathbf{s}\mathbf{s}^T + \varepsilon\mathbf{t}\mathbf{t}^T$  for  $0 < \varepsilon < 1$ , the operator

$$\mathcal{L}_M p = \nabla \cdot (M \nabla p), \quad (4.4)$$

is a rotated anisotropic diffusion operator because of the strong connection in  $\mathbf{s}$  direction. The *formal* normal equations for our problem, (4.3), result in this operator (scaled) for the limit case of  $\varepsilon = 0$ . It should be noted that the resemblance to the anisotropic diffusion equation is purely heuristic as the formulation developed in Section 2.1 uses boundary conditions typical of hyperbolic problems and not found in those of elliptic type. Multigrid techniques for the anisotropic class of diffusion operators need particular attention and a poor coarse-grid selection and inadequate intergrid transfer operators seem to require the need for more visits to the coarse grids. Our numerical tests confirm this. Unlike W-cycles, in our numerical tests V-cycles do not

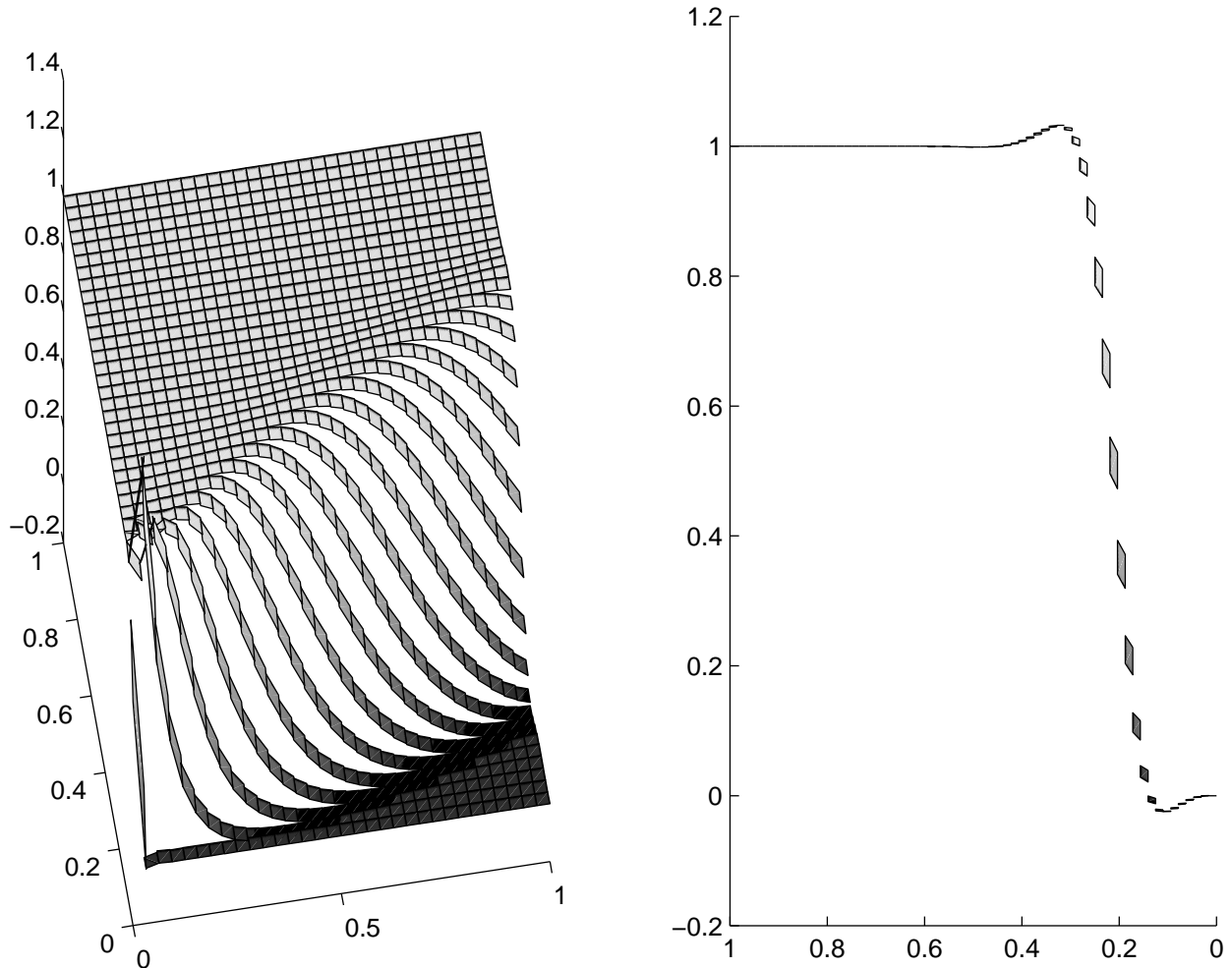


FIG. 3.2. Example solution profile for  $u$  with  $\theta = \frac{\pi}{8}$ .

handle the coarse grid well enough and result in a growth in complexity as the problem size is increased. More productive visits to coarse grids could be accomplished by more effective relaxation sweeps, although  $V(a,a)$ -cycles do not improve the performance over a  $V(1,1)$ -cycle as the number of relaxation sweeps,  $a$ , is increased.

Although the ideas presented in this section need more analysis, the preliminary results are encouraging and motivate further application in this and other contexts. The robustness of the Algebraic Multigrid enables us to easily and efficiently solve the linear system arising from a highly anisotropic problem.

**5. Concluding Remarks.** In this paper we have studied a Least-Squares Finite Element method for linear hyperbolic partial differential equations. We have formulated a “dual” problem to a conservation law and formulated the problem based on the minimization of a least-squares functional. We choose a divergence-free subspace of the Raviart-Thomas finite element space to achieve exact discrete conservation. We minimize an equivalent functional over the space of continuous piecewise bilinear elements.

Numerically we present encouraging results for this formulation. The solution quality is consistent with previous least-squares type formulations. Smearing of the discontinuities is well contained and oscillations are limited for varying meshes sizes and flow fields. Moreover, we find attractive convergence results for the finite element space as well for the desired post-processed variable  $u$ . Solving the resulting linear system can also be accomplished efficiently. Using standard Algebraic Multigrid techniques we find the complexity to remain constant as we increase the problem size.



$\theta$	N	# of cycles	Cycle complexity, $W_c$	Convergence factor, $\rho$	Work units, $W_d$
$\frac{\pi}{4}$	16	27	6.8	0.44	19.0
	32	26	7.9	0.43	21.5
	64	25	7.8	0.42	20.7
	128	24	8.3	0.40	20.8
	256	22	8.3	0.37	19.3
	512	20	8.6	0.33	18.0
$\frac{\pi}{6}$	16	19	7.7	0.30	14.6
	32	19	8.5	0.30	16.2
	64	19	9.1	0.30	17.4
	128	19	9.5	0.30	18.1
	256	19	9.6	0.30	18.3
	512	19	9.9	0.30	18.8
$\frac{\pi}{8}$	16	19	10.2	0.30	19.6
	32	19	12.7	0.30	24.4
	64	19	15.6	0.30	29.8
	128	19	16.3	0.30	31.2
	256	19	17.2	0.30	32.9
	512	19	17.8	0.30	33.9
$\frac{\pi}{12}$	16	20	9.9	0.31	19.4
	32	20	11.1	0.31	21.8
	64	20	12.3	0.30	23.6
	128	20	13.4	0.30	25.6
	256	20	13.6	0.30	26.0
	512	20	13.9	0.30	26.6

TABLE 4.1  
AMG convergence summary for  $W(1,1)$ -cycles.

The numerical investigation in this paper offers promising results and opens a variety of research potential. As we have discussed in Section 2.2, the extension to certain systems of conservation laws is straightforward. Furthermore, preliminary implementation of this framework for nonlinear conservation laws is revealing robustness in the formulation. If we consider Burger's Equation

$$\nabla \cdot \begin{pmatrix} u \\ \frac{u^2}{2} \end{pmatrix} = 0, \quad (5.1)$$

we find solution qualities similar to the linear case. Shocks are well represented discretely and conservation holds. Finally, the extension to 3-D and higher appears to follow the presentation in this paper closely when considering the equivalent sequences and operators detailed by De Rahm Cohomology [18].

#### REFERENCES

- [1] M. BERNDT, T. A. MANTEUFFEL, AND S. F. MCCORMICK, *Local error estimate and adaptive refinement for first-order system least squares (fosl)*, Electron. Trans. Numer. Anal., 6 (1997), pp. 35–43.
- [2] P. BOCHEV, J. HU, A. C. ROBINSON, AND R. TUMINARO, *Towards robust 3d z-pinch simulations: Discretization and fast solvers for magnetic diffusion in heterogeneous conductors*, tech. rep., Sandia National Laboratories, 2001. SAND Report 2001 8363J.
- [3] P. B. BOCHEV AND J. CHOI, *A comparative numerical study of least-squares, supg and galerkin methods for convection problems*, Inter. J. CFD, 00 (2001), pp. 1–21.
- [4] D. BRAESS, *Finite Elements. Theory, Fast Solvers and Applications in Solid Mechanics*, Cambridge University Press, second ed., 2001.
- [5] A. BRANDT, S. MCCORMICK, AND J. RUGE, *Algebraic multigrid (AMG) for sparse matrix equations*, in Sparsity and its applications (Loughborough, 1983), Cambridge Univ. Press, Cambridge, 1985, pp. 257–284.
- [6] S. BRENNER AND L. SCOTT, *The Mathematical Theory of Finite Element Methods*, no. 15 in Texts in Applied Mathematics, Springer-Verlag, 1994.

- [7] W. L. BRIGGS, V. E. HENSON, AND S. F. MCCORMICK, *A multigrid tutorial*, Society for Industrial and Applied Mathematics (SIAM), Philadelphia, PA, second ed., 2000.
- [8] B. COCKBURN, *Discontinuous galerkin methods for convection dominated flow*, in High order discretization methods in computational fluid dynamics, H. Deconinck and T. J. Barth, eds., Lecture notes in Computational Science and Engineering, Springer, Berlin, 1998, pp. 69–224.
- [9] H. DE STERCK, *Numerical simulation and analysis of magnetically dominated MHD bow shock flows with applications in space physics*, PhD thesis, Katholieke Universiteit Leuven (Belgium), and NationalCenter for Atmospheric Research, Boulder, Colorado (USA), 1999.
- [10] H. DE STERCK, T. A. MANTEUFFEL, S. F. MCCORMICK, AND L. OLSON, *Least-squares finite element methods for linear hyperbolic pdes*, SIAM J. Sci. Comput., (2002). submitted.
- [11] V. GIRAULT AND P.-A. RAVIART, *Finite element methods for Navier-Stokes equations*, vol. 5 of Springer Series in Computational Mathematics, Springer-Verlag, Berlin, 1986. Theory and algorithms.
- [12] P. HOUSTON, M. JENSEN, AND E. SÜLI, *hp-discontinuous galerkin finite element methods with least-squares stabilization*, tech. rep., University of Leicester, 2001.
- [13] P. HOUSTON, C. SCHWAB, AND E. SÜLI, *Stabilized hp-finite element methods for first-order hyperbolic problems*, SIAM J. Numer. Anal., 37 (2000), pp. 1618–1643.
- [14] C. JOHNSON, U. NÄVERT, AND J. PITKÄRANTA, *Finite element methods for linear hyperbolic problems*, Comput. Meth. Applied Mech. Eng., 45 (1984), pp. 285–312.
- [15] C. JOHNSON AND J. PITKÄRANTA, *An analysis of the discontinuous galerkin method for a scalar hyperbolic equation*, Math. Comp., 46 (1986), pp. 1–26.
- [16] R. J. LEVEQUE, *Numerical methods for conservation laws*, Lectures in Mathematics ETH Zurich, Birkhauser-Verlag, Basel, 1992.
- [17] J. RUGE, *FOSPACK Users Manual*, 2001. Version 1.0.
- [18] L. H. RYDER, *Quantum field theory*, Cambridge University Press, Cambridge, second ed., 1996.
- [19] E. SÜLI, P. HOUSTON, AND C. SCHWAB, *hp-finite element methods for hyperbolic problems*, tech. rep., University of Leicester, 1999.
- [20] U. TROTTEBERG, C. W. OOSTERLEE, AND A. SCHÜLLER, *Multigrid*, Academic Press Inc., San Diego, CA, 2001. With contributions by A. Brandt, P. Oswald and K. Stüben.